The role of mitochondrial oxidative stress in the metabolic alterations in diet-induced obesity in rats.

Gema Marín-Royo[1], Cristina Rodríguez[2,3], Aliaume Le Pape[1], Raquel Jurado-López[1], María Luaces[4], Alfonso Antequera[5], José Martínez-González[3,6], Francisco V Souza-Neto[1], María Luisa Nieto[3,7], Ernesto Martínez-Martínez[1,3]*, Victoria Cachofeiro[1,3]*.

[1]Departamento de Fisiología, Facultad de Medicina, Universidad Complutense de Madrid and Instituto de Investigación Sanitaria Gregorio Marañón (IiSGM), Madrid, Spain.[2] Institut de Recerca del Hospital de la Santa Creu i Sant Pau-Programa ICCC, IIB-Sant Pau, Barcelona, Spain. [3]Ciber de Enfermedades Cardiovasculares (CIBERCV). Instituto de Salud Carlos III. Madrid. Spain. [4]Servicio de Cardiología, Instituto Cardiovascular, Hospital Clínico San Carlos, Madrid, Spain. [5] Surgery Department. St Bernard's Hospital, Gibraltar, UK. [6] Instituto de Investigaciones Biomédicas de Barcelona (IIBB-CSIC), IIB-Sant Pau Barcelona, Spain.[7]Instituto de Biología y Genética Molecular, CSIC-Universidad de Valladolid, Valladolid.

*These authors contributed equally to this work.

Short Title: Mitochondrial dysfunction and obesity

Corresponding authors: V. Cachofeiro; E. Martínez-Martínez

Departamento de Fisiología, Facultad de Medicina, Universidad Complutense, Madrid 28040. Spain. Phone: 34-913941489; FAX: 34-913941628. E-mail: vcara@ucm.es; ernmarti@ucm.es

Abbreviations

CPT1A, carnitine palmitoyl transferase 1A

Cyclo F, cyclophilin F

DPP4, dipeptidylpeptidase 4

EAT, epididymal adipose tissue

ER, endoplasmic reticulum

FA, fatty acid

FAT, fatty acid translocase

FH, fumarate hydratase

GIP, glucose-dependent insulinotropic polypeptide

GLP-1, glucagon-like- peptide 1

GLUT 4, glucose transporter 4

HFD, high fat diet

HNE, hydroxynonenal

IRS-1, insulin receptor substrate-1

MFN1, Mitofusin 1

MMP 9, matrix metallopeptidase 9

MPO, myeloperoxidase

mPTP, permeability transition pores

OXPHOS, oxidative phosphorylation

PDIA6, protein disulfide isomerase A6

PRDX4, peroxiredoxin 4

ROS, reactive oxygen species

SOCS3, suppressor of cytokine signalling 3

UCP1, uncoupling protein 1

ABSTRACT

The impact of the mitochondria-targeted antioxidant MitoQ was evaluated in the metabolic alterations and the adipose tissue remodelling associated with obesity. Male Wistar rats were fed either a high fat diet (HFD, 35% fat) or a standard diet (CT, 3.5% fat) for 7 weeks and treated with MitoQ (200 μM). A proteomic analysis of visceral adipose tissue from obese and non-obese patients was performed. MitoQ partially prevented the increase in body weight, adiposity, HOMA index and adipose tissue remodelling in HFD rats. It also ameliorated protein level changes of factors involved in insulin signalling observed in adipose tissue of obese rats: reductions in adiponectin and GLUT 4, and increases in DPP4, SOCS3 and IRS-1 phosphorylation. MitoQ prevented downregulation of adiponectin and GLUT 4 and increases in SOCS3 levels in TNFα-induced insulin-resistant 3T3-L1 adipocyte model. MitoQ also ameliorated alterations in mitochondrial proteins observed in obese rats: increases in cyclophylin F and CPT1A, and reductions in mitofusin1, peroxiredoxin IV and fumarate hydratase. The proteomic analysis of the visceral adipose tissue from obese patients show alterations in mitochondrial proteins similar to those observed in obese rats. Therefore, the data show the beneficial effect of MitoQ in the metabolic dysfunction induced by obesity.

KEY WORDS: insulin resistance, mitochondrial function, obesity, oxidative stress

INTRODUCTION

Obesity is characterized by an increase in adipose tissue as a result of a positive imbalance between food intake and energy expenditure. Under conditions of constant energy surplus, adipocytes become larger in an attempt to increase their lipid storage capacity. Nonetheless, adipocytes reach a saturation point when they are not able to store more lipids and start to express stress signals (1), thereby becoming hypertrophic adipocytes. Dysfunctional adipose tissue has a negative impact on glucose homeostasis and plays a central role in the development of insulin resistance in obesity since adipose tissue serves as a crucial integrator of glucose homeostasis (2, 3).

In the last years, clinical and experimental studies have demonstrated that obesity (4-6) is associated with altered mitochondrial function in white adipose tissue, which can lead to functional consequences. Mitochondria damage is primarily caused by reactive oxygen species (ROS), with the mitochondria being the main source of ROS (7) through the oxidative phosphorylation (OXPHOS) during the process of ATP synthesis (8). In this context, selective antioxidants targeting mitochondrial ROS production are better than general antioxidants in reducing oxidative damage within mitochondria (9). Some studies have reported the relevance of mitochondrial oxidative stress in the development of some features and alterations of metabolic syndrome in muscle and liver in rats fed a high fat diet (HFD) (10, 11). However, the role played by mitochondrial oxidative stress in adipose tissue dysfunction in the context of obesity and especially in its metabolic consequences remains unclear. Therefore, the main purpose of this study was to evaluate the mitochondrial protein alterations associated with obesity in the epididymal adipose tissue (EAT) of HFD fed rats and the impact of the mitochondrial-targeted antioxidant MitoQ on the metabolic and mitochondrial alterations observed in those

animals. In addition, we have analysed the mitochondrial protein profile of visceral adipose tissue from obese patients.

MATERIAL AND METHODS

Animal model

Six week-old male Wistar rats (Envigo, Barcelona, Spain) were fed either an HFD (35% fat; Envigo no. TD.03307, Haslett, MI, USA; n=16) or a standard diet (3.5% fat; Envigo no.TD.2014, Haslett, MI, USA; n=16) for 7 weeks. Half of the animals of each group received the mitochondrial antioxidant MitoQ (200 μM) in the drinking water for the same period. The dose of MitoQ was based on previous data (12). MitoQ was provided by MP Murphy from Medical Research Council Mitochondrial Biology Unit, Cambridge BioMedical Campus, Cambridge, UK. The water intake was controlled on a daily basis to evaluate whether MitoQ was able to modify water consumption. Body weight was measured once per week. At the end of the experiment, serum and plasma were collected in fasted animals and the different fat pads (epididymal, lumbar and mesenteric adipose tissue) and brown adipose tissue were dissected for further analysis. Adiposity index was calculated as follows: sum of fat pads/[(body weight-fat pad weight)×100]. The Animal Care and Use Committee of Universidad Complutense de Madrid approved all experimental procedures according to guidelines for ethical care of experimental animals of the European Community.

Subjects

Morbidly obese patients who were referred to bariatric surgery were consecutively recruited from the Obesity Care Unit of Fuenlabrada University Hospital, Spain. The selection of the patients was performed by a multidisciplinary committee, which

includes personnel from endocrinology, general and upper gastroenterology surgery, and internal medicine and cardiology services. Inclusion criteria were age ≥18 years and universally accepted indications for bariatric surgery: long-term obesity (>4 years), body mass index ≥40 kg/m^2 despite other weight loss strategies, or body mass index ≥35 kg/m^2 in the presence of obesity-related comorbidities (diabetes mellitus, hypoventilation syndrome, obstructive sleep apnea syndrome, and hypertension). The exclusion criterion was unacceptable surgical risk because of concomitant comorbidities. Non-obese volunteers (body mass index, ≤25 kg/m^2) were recruited from staff of the hospital. Visceral adipose tissue was obtained from 10 individuals that had been referred for bariatric surgery and 10 patients that had been referred to non-bariatric surgery. The study protocol was approved by the ethics committee and all participants signed the informed consent. This study was conducted in compliance with Good Clinical Practice Guidelines and the ethical principles stated in the Declaration of Helsinki.

Cell culture and differentiation

Murine 3T3-L1 preadipocytes were cultured to confluence in DMEM (Life Technologies, Thermo Fisher Scientific Inc, Waltham, MA, USA) supplemented with 10% (v/v) calf serum (Biological Industries, Kibbutz Beit-Haemek, Israel). At 2 days post-confluence (designated day 0), cells were induced to differentiate with DMEM containing a standard induction cocktail of 10 % (v/v) fetal bovine serum (FBS; Biological Industries, Kibbutz Beit-Haemek, Israel), 1 μM dexamethasone, 0.5 mM 3-isobutyl-1-methylxanthine and 100 nM insulin (all from Sigma-Aldrich, St. Louis, MO, USA). After 48 h, this medium was replaced with DMEM supplemented with 10 % FBS and 100 nM of insulin. This medium was changed every 48 h. As a model of insulin resistance, murine TNFα (50 ng/ml, equivalent to 2.87 nM, Sigma-Aldrich, St.

Louis, MO, USA) was added to the cell culture media 7 days after the induction of differentiation, when more than 95% of the cells had the morphological and biochemical properties of adipocytes. For the TNFα treatment (72 h), fully differentiated 3T3-L1 adipocytes were treated every 24 h with the cytokine as previously described (13), MitoQ (50 nM) was added to TNFα-treated cells during the last 24 h of incubation.

Preparation of whole cell and tissue extracts

3T3-L1 preadipocytes were washed with PBS and cell monolayers were harvested in a non-denaturing buffer containing 150 mM NaCl, 10 mM Tris, pH 7.4, 1 mM EGTA, 1 mM EDTA, 1% Triton X-100, 0.5% Nonidet P-40, 1 mM Na_3VO_4, 1 µg/ml leupeptin and 1 mM DTT. Samples were extracted for 30 min on ice and centrifuged at 15,000 rpm at 4 °C for 15 min. Total proteins from EAT were obtained by homogenization in lysis buffer and centrifugation for 5 min at 13,000 rpm (4°C). The tissue extract was then separated from the fat and cellular debris and analysed for protein content. Supernatants were analysed for protein content using the BCA kit (Thermo Fisher Scientific Inc, Waltham, MA, USA).

Western blot analysis

Proteins were separated by SDS-PAGE on 12.5 % polyacrylamide gels and transferred to Hybond-c extra nitrocellulose membranes (Hybond-P; Amersham Biosciences, Piscataway, NJ, USA) with the Trans-Blot Turbo Transfer System. Membranes were probed with primary antibody for glucose transport type 4 (GLUT 4, Santa Cruz Biotechnology, Dallas, TX, USA; dilution 1/1000), adiponectin (Abcam, Cambridge, UK; dilution 1/1000), dipeptidyl-Peptidase 4 (DPP4, Abcam, Cambridge, UK; dilution 1/1000), suppressor of cytokine signaling 3 (SOCS3,Cell Signaling Technology Inc, Leiden, Netherlands; dilution 1/500), glucagon-like peptide-1 (GLP-1, Abcam,

Cambridge, UK; dilution 1/1000), IRS (*insulin* receptor substrate)-1 (Ab-636, Signalway antibody, College Park, MA, USA; dilution 1/1000), IRS-1 (Phospho-Ser636, Signalway antibody, College Park, MA, USA; dilution 1/1000), carnitine palmitoyltransferase 1A (CPT1A, Abcam; Cambridge, UK; dilution 1/500), fatty acid translocase (FAT; Abcam; Cambridge, UK; dilution 1/1000), mitofusin 1 (MFN1, Abcam; Cambridge, UK, dilution 1/1000), cyclophilin F (Cyclo F, Santa Cruz Biotechnology; Dallas, TX, USA; dilution 1/1000), peroxiredoxin 4 (PRX4, Santa Cruz Biotechnology; Dallas, TX, USA; dilution 1/1000), protein disulfide isomerise family A member 6 (PDIA6, Abcam; Cambridge, UK; dilution 1/1000), fumarate hydratase (FH; Santa Cruz Biotechno; dilution 1/ 1000) and α-tubulin, GAPDH and β-actin (Sigma-Aldrich, St Louis, MO, USA; dilution 1/5000), as loading controls. Signals were detected using the ECL system (Amersham Pharmacia Biotech, Little Chalfont, UK). Results are expressed as an n-fold increase over the values of the control group in densitometric arbitrary units.

The Mitoprofile Total OXPHOS Rodent WB Antibody Cocktail (Abcam¸ Cambridge, UK; dilution 1/1000) was used to quantify the relative levels of the subunits of the mitochondrial OXPHOS complexes: NDUFB8 subunit of complex I (20 Kda), SDHB subunit of complex II (30 kDa), core protein 2 UQCRC2 of complex III (48 kDa) MTCO1 subunit 1 of complex IV (40 kDa) and α-subunit of complex V or ATP synthase (55 kDa). For detection of OXPHOS subunits, all Western blot steps were followed.

RNA extraction from adipose tissue

Total RNA was extracted from EAT or brown adipose tissue (BAT). The extraction was carried out with Qiazol Reagent and purified using the RNeasy Lipid Tissue Kit according to the manufacturer's instructions (Qiagen, Hilden, Germany).

Reverse Transcription and Real-Time PCR

First strand cDNA was synthesized from 1.5 µg of total RNA according to the manufacturer's instructions (Go Script Reverse Transcription System, Promega; Madison, WI, USA). Quantitative PCR analysis was then performed with SYBR green PCR technology (GoTaq Real-Time PCR Systems, Promega; Madison, WI, USA) to measure uncoupling protein 1(UCP1) gene expression (Forward primer 5' to 3' CCCTGCCATTTACTGTCA; Reverse primer 5' to 3' CAGCTGGGTACACTTGGGTA3). Relative quantification was achieved with MxPro-Mx3000P software. Data were normalized by TATA BOX (Forward primer 5' to 3' CAGTACAGCAATCAACATCTAGC Reverse primer 5' to 3'CAAGTTTACAGCCAAGATTCACG) levels and expressed as percentage relative to controls. All PCRs were performed at least in triplicate for each experimental condition.

Morphological and histological evaluation

In order to detect collagen fibres, EAT samples were dehydrated, embedded in paraffin, cut into 5-µm-thick sections and stained with Picrosirius Red. The area of pericellular fibrosis was identified as the ratio of collagen deposition to the total tissue area after excluding the vessel area from the region of interest. This value was normalised by the number of adipocytes. Adipocytes (80-100 per animal) with intact cellular membranes were chosen for determination of the cross-sectional area in hematoxylin-eosin stained sections. For each sample, 10-15 fields were analysed using a 40× objective (Leica DM 2000; Leica Camera AG, Wetzlar, Germany) and quantified (Leica Q550 IWB; Leica

Camera AG, Wetzlar, Germany). A single researcher that was unaware of the experimental groups performed the analysis.

Proteomic analysis of human adipose tissue

Sample preparation for proteomic analysis

Pools of adipose tissue from obese and non-obese patients were lysed in a Precellys 24 Bead Mill Homogenizer (Bertin Technologies; Montigny-Le-Bretonneux, France) (15 x 2 s, power set to 5500 w) using 5 mM EDTA, 0.1% Triton X-100, 1% glycerol in 30 mM Hepes pH 7.4, supplemented with 1:1000 (v/v) of benzonase (Novagen; Madison, WI, USA) and 1:100 (v/v) of Halt^{TM} phosphatase and protease inhibitor cocktail 100x (Thermo Fisher Scientific, Waltham, MA; USA). Lysates were clarified by centrifugation at 4 ºC and 16000 rpm for 15 min. Recovered supernatants were cleaned-up by methanol-chloroform extraction (14).

Pellets were dissolved in 8 M urea in 0.1 M Triethylamonium bicarbonate (TEAB) buffer. Protein concentration was determined using the Bradford Protein Assay Kit (Bio-Rad, Hercules, CA, USA) using BSA as standard. Samples were then digested by means of the standard FASP protocol (15). Briefly, proteins were reduced (10 mM DTT, 30 min, RT), alkylated (50 mM IA, 20 min in the dark, RT) and sequentially digested with Lys-C protein:enzyme ratio 1:50, o/n at RT) and trypsin (Promega, Madison, WI, USA) (protein:enzyme ratio 1:100, 6 h at 37°C). Resulting peptides were desalted using C_{18} stage-tips.

Samples (110 µg) were labeled using iTRAQ® reagent 4-plex following manufacturer's instructions. Labelling scheme was as follows: Control (114) and non-diabetic morbidly obese (115). Samples were mixed in 1:1 ratios based on total peptide amount, which was determined from an aliquot by comparing overall signal intensities on a regular LC-

MS/MS run. The final mixture was finally desalted using a Sep-Pak C18 cartridge (Waters, Milford, MA, USA) and dried. The sample was reconstituted in OFFGEL solution (5% glycerol, 1% ampholytes pH 3-10) prior to electrofocusing.

Isoelectrofocusing separation

Peptides were pre-fractionated offline by means of IEF using a 3100 OFFGEL Fractionator system (Agilent Technologies, Böblingen, Germany) with a 24-well set-up. The IPG gel strips of 24 cm-long (GE Healthcare, München, Germany) with a 3–10 linear pH range were rehydrated according to the protocol provided by the manufacturer. Subsequently, 150 µL of sample was loaded in each well. Electrofocusing of the peptides was performed at 20°C and 50 µA until the 50 kVh level was reached. After focusing, the 24-peptide fractions were withdrawn and the wells rinsed with 100 µL of a solution of 0.1%TFA. Rinsing solutions were pooled with their corresponding peptide fraction. All fractions were evaporated by centrifugation under vacuum. Solid phase extraction and salt removal was performed with home–made columns based on Stage Tips with C8 Empore Disks (3M, Minneapolis, MN, USA) filled with Poros Oligo R3 resin (Life Technologies, Carlsbad, CA, USA). Eluates were evaporated to dryness and maintained at 4°C. Just prior nano-LC, the fractions were resuspended in H_2O with 0.1% (v/v) formic acid (FA).

Mass spectrometry

LC-MS/MS was done by coupling a nanoLC-Ultra 1D+ system (Eksigent) to a LTQ Orbitrap Velos mass spectrometer (ThermoFisher Scientific, Waltham, MA, USA) via a Nanospray Flex source (ThermoFisher Scientific, Waltham, MA, USA). Peptides were loaded into a trap column (ReproSil Pur C18-AQ 5 µm, 10 mm length and 0.3 mm ID, SGE Analytical, Ringwood, VIC, Australia) for 10 min at a flow rate of 2.5 µl/min in 0.1% FA. Then peptides were transferred to an analytical column (ReproSil Pur C18-

AQ 3 µm, 200 mm length and 0.075 mm ID, SGE Analytical, Ringwood, VIC, Australia) and separated using a 117 min effective linear gradient (buffer A: 4% ACN, 0.1% FA; buffer B: 100% ACN, 0.1% FA) at a flow rate of 300 nL/min. The gradient used was 0-3 min 2% B, 3-120 min 40% B, 120-131 min 98% B and 131-140 min 2% B. The peptides were electrosprayed (1.7 kV) into the mass spectrometer with a PicoTip emitter (360/20 Tube OD/ID µm, tip ID 10 µm) (New Objective), a heated capillary temperature of 240°C and S-Lens RF level of 60%. The mass spectrometer was operated in a data-dependent mode, with an automatic switch between MS and MS/MS scans using a top 15 method (threshold signal ≥ 1000 counts and dynamic exclusion of 45 sec). MS spectra (250-1750 m/z) were acquired in the Orbitrap with a resolution of 60,000 FWHM (400 m/z). Peptides were isolated using a 2 Th window and fragmented using higher-energy collisional dissociation (HCD) with Orbitrap read out at a NCE of 42% (0.25 Q-value and 0.1 ms activation time). The ion target values were 1E6 for MS (500 ms max injection time) and 2E5 for MS/MS (200 ms max injection time). Samples were injected in duplicates.

Statistical analysis

Continuous variables are expressed as mean±SD. Categorical variables are expressed in absolute values and percentages. The differences between categorical variables were analysed using the $\chi 2$ test. Normality of distributions was verified by means of the Kolmogorov–Smirnov test. Differences between 2 groups were analysed by unpaired Student t test. Specific differences between more groups were analysed using 1-way ANOVA followed by Newman-Keuls test. Pearson correlation analysis was used to examine association among different variables according to whether they are normally distributed. Multivariable analysis, considering HOMA as the dependent variable, was performed with a linear regression model by means of a backward stepwise method. In

consecutive steps, variables that were statistically significant in the univariable analysis were included in the linear regression model. A value of $P<0.05$ was used as the cutoff value for defining statistical significance. Data analysis was performed using the statistical program SPSS version 22.0 (SPSS Inc, Chicago, IL, USA).

RESULTS

HFD induced an increase in body weight that reached a significant difference with that of controls from the fifth week (Figure 1A). This difference was maintained until the end of the study. The administration of MitoQ reduced the increase in body weight, an effect that was accompanied by a decrease in white adipose tissue weight (epididymal, lumbar and mesenteric) in rats fed a HFD (Figure 1A and Table 1) and consequently reduced adiposity index (Table 1). An increase in relative BAT weight was observed in HFD as compared with CT animals (Table 1). MitoQ–treated HFD-fed rats show a slightly lower food intake as compared with HFD rats, although no significant differences were detected between both groups. However, the energy intake (calculated from the diet-contained calories) was reduced in MitoQ–treated HFD-fed rats as compared with HFD animals, although it did not reach those values observed in CT group (Table 1). To investigate whether an increase in energy expenditure is involved in the observed reduction in body weight gain, we explored the expression of UCP1, involved in energy expenditure, in BAT. Obesity only increased the expression of UCP1 in BAT from obese animals treated with MitoQ (Figure 1B). Neither HFD nor MitoQ administration were able to increase UCP1 expression in EAT, which was not detected in any animal group (data not shown).

MitoQ did not affect any of these parameters in control animals (Table 1). Therefore, and to simplify; only data from rats fed a standard diet (CT) and HFD or HFD+MitoQ will be presented from now on.

The efficiency of MitoQ treatment was evaluated by measurement of levels of protein-4-HNE adducts, a major end product of lipid peroxidation. The higher levels of 4-HNE found in EAT from HFD-fed rats were normalised with the MitoQ treatment (Figure 1C), supporting the effectiveness of MitoQ. Protein levels of both PRDX4 and FH were also reduced in HFD-fed rats and normalised with MitoQ administration (Figures 1D-1E).

Histological analysis of EAT revealed an increase in pericellular collagen content in the HFD group that was prevented by MitoQ administration (Figures 2A-2B). Pericellular collagen levels were associated with HOMA index ($r=0.495$; $P<0.031$). An increase in adipocyte area was also observed in HFD fed rats. A trend towards an attenuation of this increase due to a shift toward smaller adipocytes was observed in obese animals treated with MitoQ (Figures 2C-2E).

Considering the increase in the adiposity index and adipocyte size observed in HFD fed rats we decided to explore whether an increase in fatty acid (FA) inflow into cell and mitochondria could participate in these changes. For this purpose, we evaluated the protein levels in EAT of both the FA transporter into the cell and the FA transporter into the mitochondria, FAT and CPT1A, respectively. In HFD rats, FAT was reduced and MitoQ was unable to prevent this reduction, although it was able to prevent the increase in CPT1A observed in HFD rats (Figures 2F-2G).

Next, we examined whether the inhibition of mitochondrial oxidative stress could modify metabolic parameters in obese animals. Treatment with MitoQ improved fasted

glucose and insulin levels and consequently reduced HOMA index in the HFD group (Table 1). The levels of both 4-HNE and PRDX4 were independent predictors of HOMA (mean difference, 0.026; 95% CI, 0.003– 0.049; *P*= 0.029 and mean difference, -0.49; 95% CI, -0.88–-0.010; *P*= 0.017; respectively), supporting the relevance of oxidative stress in the development of metabolic alterations. Obese animals showed higher triglyceride levels than CT ones but no significant differences were observed in the total cholesterol (Table1). MitoQ was unable to modify lipid profile in the control group (Table 1).

In order to understand how MitoQ improves insulin sensitivity in obese animals, we analysed the levels of proteins involved in the control of insulin sensitivity in EAT. The reduction in GLUT 4, GLP-1 and adiponectin expression observed in the HFD group was normalised by MitoQ (Figures 3A-3C). Furthermore, the increase in the protein levels of DPP4 and SOCS3 triggered by the HFD was completely prevented by MitoQ, which was also able to ameliorate the increase in the phosphorylation of Ser (*636*) of IRS-1 (Figures 3D-3F). To determine whether MitoQ could directly affect adipocyte function, we carried out *in vitro* experiments in the TNFα-induced insulin resistance model in differentiated 3T3-L1 adipocytes. As shown in Figure 4 and as previously described (13), TNFα reduced GLUT 4 and adiponectin expression and increased SOCS3 protein levels in these cells. Interestingly, these effects were prevented by MitoQ (Figures 4A-4C).

Regarding mitochondrial markers, protein levels of mitochondrial complexes I, II and IV were reduced, while complex V was increased in HFD-fed rats (Figure 5A). MitoQ treatment was only able to reduce the increase in complex V. Complex III was altered neither in HFD nor in HFD + MQ rats. Obesity was also able to increase Cyclo F levels (Figure 5B), suggesting the opening of the mitochondrial permeability transition pores

(mPTP), which was normalized by MitoQ treatment. MFN1, a protein involved in the mitochondrial fusion process, was reduced in HFD rats and was prevented in those treated with MitoQ (Figure 5C). MFN1 was an independent predictor of HOMA index (mean difference, 0.058; 95% CI, 0.004– 0.113; *P*= 0.038). We also assessed the levels of PDIA6, a marker of endoplasmic reticulum (ER) stress. PDIA6 levels were higher in HFD rats than in controls and this increase was prevented in those HFD rats treated with MitoQ (Figure 5D).

In order to verify whether the adipose tissue remodelling occurs not only in an obese animal model but also in obese patients, we performed a proteomic study of adipose tissue from control and obese (non-diabetic) subjects. The mean age of both groups was similar, with there being more women in the group of obese patients (Table 2). The majority of obese patients, but only 17.9% of the lean subjects, had associated comorbidities with the most hypertension and dyslipidemia (Table 2). Drug treatment for hypertension included angiotensin converting enzyme inhibitors (or angiotensin II type 1 receptor antagonists), whereas all dyslipidemic patients were on statins. Body mass index (BMI), fasting plasma glucose and insulin levels and HOMA index were higher in obese than in non-obese subjects, as occurs in the obese rats (Table 2).

Histological analysis of visceral adipose tissue showed an enhanced adipocyte area (Figure 6A) and an increase in pericellular collagen (Figure 6B) in obese patients as compared with control subjects. As shown in Table 2, obese patients had higher serum levels of inflammatory markers, including C-reactive protein, interleukin (IL) 1β, IL6 tumor necrosis factor-α, and MMP 9 than lean subjects, although no differences were observed in the anti-inflammatory cytokine IL10. Obese patients also showed an increase in MPO, a marker of oxidative stress. As compared with non-obese subjects, obese patients showed a reduction in levels of adiponectin and ghrelin but no changes

were observed in those of GLP-1 and GIP, and leptin plasma levels were significantly increased. The anthropometrical and clinical characteristics of the patients used for the proteomic analysis of the adipose tissue follow the same pattern observed for the all patients included in the study, suggesting that they are a representative sample - (data not shown).

2119 proteins were identified in the proteomic analysis of human adipose tissue, of which 53 were related to mitochondria. Those proteins with a fold change > 1.3 (up-regulation) or <0.769 (down-regulation) between obese and control group were selected. According to these criteria, 23 of the 53 mitochondrial proteins were modified in the obese patients (Table 3).

Most of the modified mitochondrial proteins were involved in FA β-oxidation, Krebs cycle or OXPHOS. Six proteins involved in FA β-oxidation and Krebs cycle were reduced in obese patients as compared with controls, suggesting an impaired metabolism. OXPHOS proteins were altered (five reduced and two increased) in obese patients. Two subunits of the mitochondrial complex I: NADH dehydrogenase [ubiquinone] flavoprotein 1 and NADH dehydrogenase [ubiquinone] flavoprotein 2) were reduced in obese patients, which were also reduced in EAT of HFD rats. On the other hand, a subunit of mitochondrial complex V or ATPase (described in Table 3 as ATP synthase lipid-binding protein) was increased in obese patients as compared with lean subjects, and as occurs in the EAT of obese rats.

DISCUSSION

The results presented here reveal that the metabolic alterations observed in diet-induced obesity were accompanied by an exacerbation of oxidative stress, remodelling and mitochondrial proteins alterations in adipose tissue. We hypothesized that mitochondrial

oxidative stress could participate in metabolic alterations associated with obesity. Interestingly, we observed that the administration of the mitochondrial antioxidant MitoQ protects against some of the consequences of diet-induced obesity, thereby limiting weight gain, attenuating the disturbances in adipose tissue and improving the insulin resistance observed in obese animals.

HFD-fed animals exhibited a decline in insulin sensitivity, a common feature in obese patients, as indicated by an increase in HOMA index. Alterations in the balance of factors that modulate (increase/decrease) insulin sensitivity seems to underlie the dysfunctional glucose homeostasis observed in obese rats. Such alterations included reduced levels of GLUT 4, adiponectin and GLP-1, as well as increased levels of DPP4, SOCS3 and IRS-1 serine phosphorylation. Similar results have previously been described in both humans and animal models (13, 16-18). The relevance of SOCS3 in insulin resistance is confirmed by the fact that their levels were independently associated with HOMA index. All of these alterations were improved by MitoQ treatment showing the role of mitochondrial oxidative stress on insulin sensitivity (10, 19).

An increase in oxidative stress seems to be involved in insulin resistance in HFD-fed rats since HOMA index was associated with 4-HNE levels. This bioreactive aldehyde is not only a byproduct of lipid peroxidation, but is also able to induce oxidative stress and contribute to adipose tissue metabolic dysfunction associated with insulin resistance in human adipocytes (20). Other sources of free radicals in addition to mitochondria could participate in the oxidative environment observed in obese rats since FH levels were decreased in HFD rats and associated with those of 4-HNE. The decrease in FH levels can allow a consequent rise in fumarate production, which is involved in ROS generation (21, 22). In addition, a reduction in antioxidant defence could also participate

since levels of PRDX4, which metabolize hydrogen peroxide, were reduced in adipose tissue of obese rats. These results agree with a previous study, which observed a reduction in the activity of antioxidant enzymes parallel to the increase in adipose tissue (23). MitoQ was able to reverse the reduction in both FH and PRDX4, supporting the complexity of the effects of this antioxidant in the modulation of oxidative stress. More relevant is the fact that levels of both PRDX4 and 4-HNE were independently associated with HOMA index, supporting the importance of oxidative stress in adipocyte function. In addition, levels of MFN1 were independent predictors of HOMA index, confirming previous observations, which show an interaction between mitochondria dynamics and insulin resistance (24, 25).

Pericellular fibrosis seems to be an additional mechanism involved in insulin resistance in HFD rats since it was associated with HOMA index, and the improvement in insulin sensitivity in MitoQ-treated rats was accompanied by a decrease in pericellular fibrosis. The observation of a reduction in FAT levels, a protein involved in FA inflow inside cell, suggests a maladaptive response to excess dietary FA that may facilitate ectopic fat deposit (26) and MitoQ was unable to affect it. In agreement with that observation, MitoQ was unable to normalize the enlarged adipocytes in obese rats.

Obesity is also accompanied by changes in levels of different mitochondrial proteins in EAT: Cyclo F and MFN1 which are involved in essential processes which can affect mitochondrial survival (27, 28) leading to cell death (29). MitoQ treatment was able to normalize the levels of Cyclo F and MFN1, suggesting that oxidative stress seems to be involved in the regulation of these two essential processes: opening and regulation of mPTP, and mitochondrial fusion. Moreover, obesity is also accompanied by ER stress activation as suggested by the increase in PDIA6 levels, which was reduced in MitoQ-treated rats. In fact, ER stress can further damage mitochondria by regulating mPTP

opening through an increase in Ca^{2+} levels and further aggravate oxidative stress by augmenting ROS production in ER (30), which can also be potentiated by the reduction in the antioxidant PRDX4, which is mainly localized in ER.

In accordance with previous studies (10, 31, 32) a reduction in energy intake could be involved in the slimming effect induced by MitoQ in HFD rats. In addition, an increase in energy expenditure could also be proposed in the observed body weight reduction. This affirmation is based on the fact that MitoQ treatment was associated with an increase in levels of UCP1, which dissipates energy as heat, in brown adipose tissue of HFD rats, supporting the capacity of MitoQ in increase uncoupling oxidative phosphorylation from ATP synthesis (32, 33). Previous studies have reported that proliferator-activated receptor γ (PPAR γ) is involved in energy expenditure since treatment with PPAR γ agonists is accompanied by a strong induction of UCP-1 mRNA expression which is associated with a reduction in body weight in mice (34-36). In this regard, we have observed in preliminary data that MitoQ treatment was able to reverse the reduction in PPARγ induced by HFD (data not shown).

Considering the reduction in body weight observed during MitoQ treatment, we cannot exclude the possibility that this MitoQ-elicited reduction in HFD-fed animals could also be partially responsible for improvement in insulin resistance in these animals. However, although MitoQ-treated rats normalized insulin sensitivity, they showed a higher adiposity and enlarged adipocytes relative to control animals. Moreover, MitoQ normalized GLUT 4, adiponectin and SOCS3 expression in cultured adipocytes, supporting a direct effect of this compound in adipose tissue glucose signaling. This effect could involve not only mitochondrial redox regulation but also lipid metabolism modulation (10). In fact, we have found an increase in CPT1A in MitoQ-treated animals, supporting an increase in β-oxidation.

Obese patients showed a low-grade systemic inflammation and a prooxidant state, a fact amply reported in the literature (37-40). This proinflammatory and prooxidant environment has been explained by dysfunctional adipose tissue that occurred in the context of obesity. Accordingly, and similar to that observed in rats, obese patients show a remodelling of visceral adipose tissue characterized by adipocyte hypertrophy and increased deposition of extracellular matrix, confirming previous observations (13). In addition, the proteomic analysis of the visceral adipose tissue shows important changes, including at mitochondrial level, since almost 50% of the mitochondrial proteins identified were modified in obese patients, suggesting that obesity exerts an important impact on mitochondria. Such proteins were involved in metabolism (β-oxidation and citric acid cycle), which were showed to be reduced as compared with normoweight individuals and OXPHOS proteins (subunits of complex I which were reduced and a subunit of complex V which was increased) showing a similar pattern to the one observed in obese rats. Likewise, there have been reported alterations in the genes involved in metabolism, as well as OXPHOS in subcutaneous adipose tissue of obese patients with type 2 diabetes mellitus. A decrease in proteins involved in metabolism, as well as a decrease in activity of complex I and V was found in abdominal adipose tissue of obese children (41). These data suggest that obesity is associated with mitochondrial and structure alterations in the adipose tissue.

The results obtained in obese human samples reveal that some of the alterations observed in the EAT of obese rats are also reflected in the visceral adipose tissue of obese patients, further suggesting the clinical relevance of our findings. These alterations include oxidative parameters such as PRDX, ER stress markers like PDIA6, HOMA index and circulating factors involved in insulin sensitivity including GIP, adiponectin and ghrelin.

Conclusions

In summary, this study demonstrates the beneficial effect of the mitochondrial antioxidant MitoQ in the metabolic alterations associated with obesity. Although additional mechanisms could not be ruled out, our data emphasize the interest of mitochondrial ROS as a potential therapeutic target in obesity and highlight the benefits of mitochondrial-targeted antioxidant drugs for this disease.

Limitations of the study

Although the study explores the potential role of mitochondrial oxidative stress in the adipose tissue remodelling and the metabolic alterations observed in obesity, the assessment of mitochondrial function was derived from the evaluation of protein levels involved in essential mitochondrial processes, and this represents a limitation of our study. In addition, we have used the surrogate marker HOMA index for the evaluation of insulin sensitivity in spite of direct assessments for evaluation of insulin sensitivity such as the glucose clamp technique. Although HOMA index is considered to be a useful tool to estimate insulin resistance, simple tests involving a single fasting blood sample could be a limitation of the study. Another notable consideration related to the study is the fact that MitoQ is a mitochondrial targeting antioxidant with a ubiquinone moiety attached to a dTPP+ cation. In a recent paper, it has been described that the lipophilic cation moiety triphenylphosphonium (TPP+) of MitoQ can mediate some of the observed effects of this antioxidant (33). For this reason, we cannot preclude which moiety of the MitoQ molecule could exert the beneficial effects described in the manuscript since we did not use animals treated with TPP+ as controls.

Acknowledgments

We thank Avelina Hidalgo, Blanca Martínez, Virginia Peinado, and Roberto Cañadas for their technical help. We thank to Isabel Ruppen, Javier Muñoz and Pilar Ximénez-Embún from the Proteomics Unit of the CNIO, which belongs to ProteoRed, PRB2-ISCIII, supported by grant PT13/0001. We thank Anthony DeMarco for his help in editing.

This work was supported by Instituto de Salud Carlos III-Fondo Europeo de Desarrollo Regional (FEDER) (PI15/01060, PI18/00257, PI18/0919 and; CIBERCV) a way to build Europe, Ministerio de Economia y Competitividad (SAF2016-81063**)** and Agencia de Gestio d'Ajuts Universitaris i de Recerca (AGAUR; program of Support to Research Groups, Ref. 2017-SGR-00333). EM-M was supported by a contract from CAM (Atracción de talento). MitoQ was provided by MP Murphy from Medical Research Council Mitochondrial Biology Unit, Cambridge BioMedical Campus, Cambridge, UK.

Author Contributions

GM-R, AL-P performed animal experiments, data analysis and helped to write the manuscript. RJ-L and FVS-N performed animal experiments, circulating parameter measurements, and data analysis. CR and JM-G performed cell culture studies, data analysis and helped to write the manuscript. ML and AA performed clinical study, data analysis and helped to write the manuscript. MLN contributed to measurement of circulating parameter, data analysis and helped to write the manuscript. EM-M and VC designed the study, performed experiments, data analysis and wrote the manuscript.

Disclosure Statement

The authors have no conflicts of interest to declare.

References

1. Haczeyni, F., Bell-Anderson, K. S., and Farrell, G. C. (2018) Causes and mechanisms of adipocyte enlargement and adipose expansion. *Obes Rev* **19**, 406-420
2. Goossens, G. H. (2008) The role of adipose tissue dysfunction in the pathogenesis of obesity-related insulin resistance. *Physiol Behav* **94**, 206-218
3. Guilherme, A., Virbasius, J. V., Puri, V., and Czech, M. P. (2008) Adipocyte dysfunctions linking obesity to insulin resistance and type 2 diabetes. *Nat Rev Mol Cell Biol* **9**, 367-377
4. Yin, X., Lanza, I. R., Swain, J. M., Sarr, M. G., Nair, K. S., and Jensen, M. D. (2014) Adipocyte mitochondrial function is reduced in human obesity independent of fat cell size. *J Clin Endocrinol Metab* **99**, E209-216
5. Heinonen, S., Buzkova, J., Muniandy, M., Kaksonen, R., Ollikainen, M., Ismail, K., Hakkarainen, A., Lundbom, J., Lundbom, N., Vuolteenaho, K., Moilanen, E., Kaprio, J., Rissanen, A., Suomalainen, A., and Pietilainen, K. H. (2015) Impaired Mitochondrial Biogenesis in Adipose Tissue in Acquired Obesity. *Diabetes* **64**, 3135-3145
6. Rong, J. X., Qiu, Y., Hansen, M. K., Zhu, L., Zhang, V., Xie, M., Okamoto, Y., Mattie, M. D., Higashiyama, H., Asano, S., Strum, J. C., and Ryan, T. E. (2007) Adipose mitochondrial biogenesis is suppressed in db/db and high-fat diet-fed mice and improved by rosiglitazone. *Diabetes* **56**, 1751-1760
7. Wei, Y. H., Lu, C. Y., Lee, H. C., Pang, C. Y., and Ma, Y. S. (1998) Oxidative damage and mutation to mitochondrial DNA and age-dependent decline of mitochondrial respiratory function. *Ann N Y Acad Sci* **854**, 155-170

8. Bhatti, J. S., Bhatti, G. K., and Reddy, P. H. (2017) Mitochondrial dysfunction and oxidative stress in metabolic disorders - A step towards mitochondria based therapeutic strategies. *Biochim Biophys Acta* **1863**, 1066-1077
9. Kelso, G. F., Porteous, C. M., Coulter, C. V., Hughes, G., Porteous, W. K., Ledgerwood, E. C., Smith, R. A., and Murphy, M. P. (2001) Selective targeting of a redox-active ubiquinone to mitochondria within cells: antioxidant and antiapoptotic properties. *J Biol Chem* **276**, 4588-4596
10. Feillet-Coudray, C., Fouret, G., Ebabe Elle, R., Rieusset, J., Bonafos, B., Chabi, B., Crouzier, D., Zarkovic, K., Zarkovic, N., Ramos, J., Badia, E., Murphy, M. P., Cristol, J. P., and Coudray, C. (2014) The mitochondrial-targeted antioxidant MitoQ ameliorates metabolic syndrome features in obesogenic diet-fed rats better than Apocynin or Allopurinol. *Free Radic Res* **48**, 1232-1246
11. Coudray, C., Fouret, G., Lambert, K., Ferreri, C., Rieusset, J., Blachnio-Zabielska, A., Lecomte, J., Ebabe Elle, R., Badia, E., Murphy, M. P., and Feillet-Coudray, C. (2016) A mitochondrial-targeted ubiquinone modulates muscle lipid profile and improves mitochondrial respiration in obesogenic diet-fed rats. *Br J Nutr* **115**, 1155-1166
12. Rivera-Barahona, A., Alonso-Barroso, E., Perez, B., Murphy, M. P., Richard, E., and Desviat, L. R. (2017) Treatment with antioxidants ameliorates oxidative damage in a mouse model of propionic acidemia. *Mol Genet Metab* **122**, 43-50
13. Miana, M., Galan, M., Martinez-Martinez, E., Varona, S., Jurado-Lopez, R., Bausa-Miranda, B., Antequera, A., Luaces, M., Martinez-Gonzalez, J., Rodriguez, C., and Cachofeiro, V. (2015) The lysyl oxidase inhibitor beta-aminopropionitrile reduces body weight gain and improves the metabolic profile in diet-induced obesity in rats. *Dis Model Mech* **8**, 543-551

14. Kline, K. G., Frewen, B., Bristow, M. R., Maccoss, M. J., and Wu, C. C. (2008) High quality catalog of proteotypic peptides from human heart. *J Proteome Res* **7**, 5055-5061
15. Wisniewski, J. R., Zougman, A., Nagaraj, N., and Mann, M. (2009) Universal sample preparation method for proteome analysis. *Nat Methods* **6**, 359-362
16. Kadowaki, T., Yamauchi, T., Kubota, N., Hara, K., Ueki, K., and Tobe, K. (2006) Adiponectin and adiponectin receptors in insulin resistance, diabetes, and the metabolic syndrome. *J Clin Invest* **116**, 1784-1792
17. Lamers, D., Famulla, S., Wronkowitz, N., Hartwig, S., Lehr, S., Ouwens, D. M., Eckardt, K., Kaufman, J. M., Ryden, M., Muller, S., Hanisch, F. G., Ruige, J., Arner, P., Sell, H., and Eckel, J. (2011) Dipeptidyl peptidase 4 is a novel adipokine potentially linking obesity to the metabolic syndrome. *Diabetes* **60**, 1917-1925
18. Palanivel, R., Fullerton, M. D., Galic, S., Honeyman, J., Hewitt, K. A., Jorgensen, S. B., and Steinberg, G. R. (2012) Reduced Socs3 expression in adipose tissue protects female mice against obesity-induced insulin resistance. *Diabetologia* **55**, 3083-3093
19. Jeong, E. M., Chung, J., Liu, H., Go, Y., Gladstein, S., Farzaneh-Far, A., Lewandowski, E. D., and Dudley, S. C., Jr. (2016) Role of Mitochondrial Oxidative Stress in Glucose Tolerance, Insulin Resistance, and Cardiac Diastolic Dysfunction. *J Am Heart Assoc* **5**
20. Elrayess, M. A., Almuraikhy, S., Kafienah, W., Al-Menhali, A., Al-Khelaifi, F., Bashah, M., Zarkovic, K., Zarkovic, N., Waeg, G., Alsayrafi, M., and Jaganjac, M. (2017) 4-hydroxynonenal causes impairment of human subcutaneous adipogenesis and induction of adipocyte insulin resistance. *Free Radic Biol Med* **104**, 129-137

21. Ibarrola, J., Sadaba, R., Garcia-Pena, A., Arrieta, V., Martinez-Martinez, E., Alvarez, V., Fernandez-Celis, A., Gainza, A., Santamaria, E., Fernandez-Irigoyen, J., Cachofeiro, V., Fay, R., Rossignol, P., and Lopez-Andres, N. (2018) A role for fumarate hydratase in mediating oxidative effects of galectin-3 in human cardiac fibroblasts. *Int J Cardiol* **258**, 217-223
22. Tian, Z., Liu, Y., Usa, K., Mladinov, D., Fang, Y., Ding, X., Greene, A. S., Cowley, A. W., Jr., and Liang, M. (2009) Novel role of fumarate metabolism in dahl-salt sensitive hypertension. *Hypertension* **54**, 255-260
23. Fernandez-Sanchez, A., Madrigal-Santillan, E., Bautista, M., Esquivel-Soto, J., Morales-Gonzalez, A., Esquivel-Chirino, C., Durante-Montiel, I., Sanchez-Rivera, G., Valadez-Vega, C., and Morales-Gonzalez, J. A. (2011) Inflammation, oxidative stress, and obesity. *Int J Mol Sci* **12**, 3117-3132
24. Kavanagh, K., Davis, A. T., Peters, D. E., LeGrand, A. C., Bharadwaj, M. S., and Molina, A. J. (2017) Regulators of mitochondrial quality control differ in subcutaneous fat of metabolically healthy and unhealthy obese monkeys. *Obesity (Silver Spring)* **25**, 689-696
25. Tol, M. J., Ottenhoff, R., van Eijk, M., Zelcer, N., Aten, J., Houten, S. M., Geerts, D., van Roomen, C., Bierlaagh, M. C., Scheij, S., Hoeksema, M. A., Aerts, J. M., Bogan, J. S., Dorn, G. W., 2nd, Argmann, C. A., and Verhoeven, A. J. (2016) A PPARgamma-Bnip3 Axis Couples Adipose Mitochondrial Fusion-Fission Balance to Systemic Insulin Sensitivity. *Diabetes* **65**, 2591-2605
26. McQuaid, S. E., Hodson, L., Neville, M. J., Dennis, A. L., Cheeseman, J., Humphreys, S. M., Ruge, T., Gilbert, M., Fielding, B. A., Frayn, K. N., and Karpe, F. (2011) Downregulation of adipose tissue fatty acid trafficking in obesity: a driver for ectopic fat deposition? *Diabetes* **60**, 47-55

27. Rovira-Llopis, S., Banuls, C., Diaz-Morales, N., Hernandez-Mijares, A., Rocha, M., and Victor, V. M. (2017) Mitochondrial dynamics in type 2 diabetes: Pathophysiological implications. *Redox Biol* **11**, 637-645
28. Lopez-Lluch, G. (2017) Mitochondrial activity and dynamics changes regarding metabolism in ageing and obesity. *Mech Ageing Dev* **162**, 108-121
29. Feng, D., Tang, Y., Kwon, H., Zong, H., Hawkins, M., Kitsis, R. N., and Pessin, J. E. (2011) High-fat diet-induced adipocyte cell death occurs through a cyclophilin D intrinsic signaling pathway independent of adipose tissue inflammation. *Diabetes* **60**, 2134-2143
30. Ly, L. D., Xu, S., Choi, S. K., Ha, C. M., Thoudam, T., Cha, S. K., Wiederkehr, A., Wollheim, C. B., Lee, I. K., and Park, K. S. (2017) Oxidative stress and calcium dysregulation by palmitate in type 2 diabetes. *Exp Mol Med* **49**, e291
31. Fink, B. D., Herlein, J. A., Guo, D. F., Kulkarni, C., Weidemann, B. J., Yu, L., Grobe, J. L., Rahmouni, K., Kerns, R. J., and Sivitz, W. I. (2014) A mitochondrial-targeted coenzyme q analog prevents weight gain and ameliorates hepatic dysfunction in high-fat-fed mice. *J Pharmacol Exp Ther* **351**, 699-708
32. Imai, Y., Fink, B. D., Promes, J. A., Kulkarni, C. A., Kerns, R. J., and Sivitz, W. I. (2018) Effect of a mitochondrial-targeted coenzyme Q analog on pancreatic beta-cell function and energetics in high fat fed obese mice. *Pharmacol Res Perspect* **6**, e00393
33. Bond, S. T., Kim, J., Calkin, A. C., and Drew, B. G. (2019) The Antioxidant Moiety of MitoQ Imparts Minimal Metabolic Effects in Adipose Tissue of High Fat Fed Mice. *Front Physiol* **10**, 543
34. Kelly, L. J., Vicario, P. P., Thompson, G. M., Candelore, M. R., Doebber, T. W., Ventre, J., Wu, M. S., Meurer, R., Forrest, M. J., Conner, M. W., Cascieri, M. A.,

and Moller, D. E. (1998) Peroxisome proliferator-activated receptors gamma and alpha mediate in vivo regulation of uncoupling protein (UCP-1, UCP-2, UCP-3) gene expression. *Endocrinology* **139**, 4920-4927

35. Fukui, Y., Masui, S., Osada, S., Umesono, K., and Motojima, K. (2000) A new thiazolidinedione, NC-2100, which is a weak PPAR-gamma activator, exhibits potent antidiabetic effects and induces uncoupling protein 1 in white adipose tissue of KKAy obese mice. *Diabetes* **49**, 759-767
36. Sell, H., Berger, J. P., Samson, P., Castriota, G., Lalonde, J., Deshaies, Y., and Richard, D. (2004) Peroxisome proliferator-activated receptor gamma agonism increases the capacity for sympathetically mediated thermogenesis in lean and ob/ob mice. *Endocrinology* **145**, 3925-3934
37. Frasca, D., Blomberg, B. B., and Paganelli, R. (2017) Aging, Obesity, and Inflammatory Age-Related Diseases. *Front Immunol* **8**, 1745
38. Heilbronn, L. K., and Campbell, L. V. (2008) Adipose tissue macrophages, low grade inflammation and insulin resistance in human obesity. *Curr Pharm Des* **14**, 1225-1230
39. Fruhbeck, G., Catalan, V., Rodriguez, A., Ramirez, B., Becerril, S., Salvador, J., Portincasa, P., Colina, I., and Gomez-Ambrosi, J. (2017) Involvement of the leptin-adiponectin axis in inflammation and oxidative stress in the metabolic syndrome. *Sci Rep* **7**, 6619
40. Monzo-Beltran, L., Vazquez-Tarragon, A., Cerda, C., Garcia-Perez, P., Iradi, A., Sanchez, C., Climent, B., Tormos, C., Vazquez-Prado, A., Girbes, J., Estan, N., Blesa, S., Cortes, R., Chaves, F. J., and Saez, G. T. (2017) One-year follow-up of clinical, metabolic and oxidative stress profile of morbid obese patients after

laparoscopic sleeve gastrectomy. 8-oxo-dG as a clinical marker. *Redox Biol* **12**, 389-402

41. Zamora-Mendoza, R., Rosas-Vargas, H., Ramos-Cervantes, M. T., Garcia-Zuniga, P., Perez-Lorenzana, H., Mendoza-Lorenzo, P., Perez-Ortiz, A. C., Estrada-Mena, F. J., Miliar-Garcia, A., Lara-Padilla, E., Ceballos, G., Rodriguez, A., Villarreal, F., and Ramirez-Sanchez, I. (2018) Dysregulation of mitochondrial function and biogenesis modulators in adipose tissue of obese children. *Int J Obes (Lond)* **42**, 618-624

Figure Legends

Figure 1. (A) Body weight evolution along the study. **(B)** UCP1 mRNA levels in brown adipose tissue. Protein levels of **(C)** 4-hydroxynonenal (4-HNE) adducts**,** (**D)** peroxiredoxin 4 (PRX4) and **(E)** fumarate hydratase (FH) in epididymal adipose tissue from control rats fed a normal chow (CT) and rats fed a high fat diet (HFD) treated with vehicle or with the mitochondrial antioxidant MitoQ (MQ; 200 µM). Bars graphs represent the mean ± SD of 6-8 animals normalized for reference housekeeping**.** * $p<0.05$, **$p<0.01$ *vs.* control group. $^{\dagger}p<0.05$, $^{\dagger\dagger}p<0.01$ *vs.* HFD group.

Figure 2. (A and B) Quantification of collagen volume fraction normalized for adipocyte number (CVF) and representative microphotographs of epididymal adipose tissue from fed a normal chow (CT) and animals fed a high fat diet (HFD) treated with vehicle or with the mitochondrial antioxidant MitoQ (MQ; 200 µM) stained with picrosirius red examined by light microscopy (magnification 20X). **(C and E)** Quantification and size distribution of adipocytes from epididymal of adipocyte area and representative microphotographs of epididymal adipose tissue from CT and HFD rats stained with haematoxylin eosin examined by light microscopy (magnification 20X). **(F and G)** Protein levels of FA translocase (FAT) and carnitine palmitoyltransferase 1A (CPT1A), respectively in epididymal adipose tissue from control rats fed a normal chow (CT) and rats fed a HFD treated with vehicle or with the mitochondrial antioxidant MitoQ (MQ; 200 µM). Scale bar: 100 µm. Values are mean± SD of 6-8 animals. **$p<0.01$; *** $p<0.001$ *vs.* control group. $^{\dagger}p<0.05$; $^{\dagger\dagger\dagger}p<0.001$ *vs.* HFD group.

Figure 3. Protein levels of **(A)** Glucose transporter type 4 (GLUT 4), **(B)** glucagon-like peptide-1 (GLP-1), **(C)** adiponectin, **(D)** Dipeptidylpeptidase 4 (DPP4), **(E)** suppressor

of cytokine signalling 3 (SOCS3) and **(F)** insulin receptor substrate-1 (IRS-1; total and phosphorylated forms) in epididymal adipose tissue from control rats fed a normal chow (CT) and rats fed a high fat diet (HFD) treated with vehicle or with the mitochondrial antioxidant MitoQ (MQ; 200 μM). Bars graphs represent the mean ± SD of 6-8 animals normalized to for reference housekeeping. **p<0.01; *** p<0.001 *vs.* control group. †p<0.05, †† p<0.01 *vs* HFD group.

Figure 4. Protein levels of **(A)** Glucose transporter type 4 (GLUT 4), **(B)** adiponectin and **(C)** suppressor of cytokine signalling 3 (SOCS3) in 3T3-L1 adipocytes. The cells were stimulated with or withouth TNFα (50 ng/mL) for 72 h in the presence of either vehicle or the mitochondrial antioxidant MitoQ (MQ; 5 nM). Data normalized to β-actin are expressed as mean ± SD of four assays in arbitrary units. *p<0.05, **p<0.01, *vs.* unstimulated cells (CT); †p<0.05, cells stimulated with the same concentration of TNFα in the absence of MitoQ.

Figure 5. Protein levels of **(A)** mitochondrial complexes I-V, **(B)** cyclophilin F (Cyclo F), **(C)** mitofusin (MFN1), and (**D)** protein disulfide isomerise family A member 6 (PDIA6) in epididymal adipose tissue from control rats fed a normal chow (CT) and rats fed a high fat diet (HFD) treated with vehicle or with the mitochondrial antioxidant MitoQ (MQ; 200 μM). Bars graphs represent the mean ± SD of 6-8 animals normalized to for reference housekeeping. *p<0.05, **p<0.01; *** p<0.001 *vs.* control group. †p<0.05, †† p<0.01 *vs* HFD group.

Figure 6. (A) Quantification of adipocyte area (left) and representative microphotographs of visceral adipose tissue sections from control subjects (CT) and morbidly obese patients (OB) stained with haematoxylin eosin examined by light microscopy (magnification 20X; right), **(B)** Quantification of collagen volume fraction normalized for adipocyte number (CVF). Right panel shows representative

microphotographs of visceral adipose tissue sections from these individuals stained with picrosirius redexamined by light microscopy (magnification 20X). Bars histograms represent the mean ± SD of 7 subjects. Scale bar: 100 µm. ** $p<0.01$ *vs.* control group.

Table 1. Effect of the mitochondrial antioxidant MitoQ (200 µM) on general characteristics and metabolic parameters in rats fed a normal chow (CT) and high fat diet (HFD) fed rats

	CT	MitoQ	HFD	HFD+MitoQ
F I (g/day)	22.3±1.5	21.2±1.6	18.6±3.1**	16.0±2.1***
EI (kcal)	64.7±4.3	61.5±4.0	100.4±16.7***	86.4±11.3***†
WI (mL/day)	42.3±7.1	48.0±8.5	41.8±5.6	43.9±1.0
EAT (g/cm tibia)	1.1±0.35	0.09±0.21	3.18±0.91***	2.3±0.54**†
LAT (g/cm tibia)	1.81±0.49	1.76±0.43	3.86±0.81***	2.77±0.31*††
MAT (g/cm tibia)	0.85±0.24	0.82±0.12	1.84±0.27**	1.44±0.17***††
Adiposity Index (%)	4.6±1.13	4.2±0.83	9.1±1.01***	7.8±0.85***†
BAT (g/cm tibia)	0.126±0.03	0.136±0.015	0.184±0.05*	0.166±0.012*
Glucose(mg/dl)	96.5±11.4	99.6±11.7	115.4±6.3*	100.3±10.34†
Insulin (pg/ml)	90.8±15.2	79.3±20.4	272.3±90.4***	153.6±36.8*††
HOMA Index	3.3±1.4	2.9±1.3	10.3±4.2***	5.4±2.5††
TG (mg/dl)	78.6±15.6	89.7±18.3	146.8±32.9*	129.0±35.9*
TC (mg/dl)	66.5±14.8	68.2±10.5	68.1±10.9	68.8±8.4

BAT: brown adipose tissue; BW: body weight; EAT: epididymal adipose tissue; EI: energy intake; FI: food intake; HOMA index: the homeostasis model assessment; LAT: lumbar adipose tissue; MAT: mesenteric adipose tissue TG: triglycerides and TC: total Cholesterol: WI: water intake. Data values represent mean ± SD of 8 animals. *p < 0.05 compared to control group. * p<0.05; **p < 0.01; *** p<0.001 compared to control group. †p0.05, ††p<0.01; †††p<0.001 compared to HFD group.

TABLE 2. Epidemiological and clinical characteristics and circulating markers of morbidly obese patients and lean subjects.

	Lean Subjects, n=67	Obese patients, n=63	*P* Value
Age (years)	41.4 ±5.11	40.4 ±9.48	0.435
Women (%)	30	40.3	0.004
BMI (kg/m^2)	22.8±1.97	45.8±5.44	<0.0001
Comorbidities (n, %)	11 (16.5%)	55 (87.3%)	<0.001
Hypertension (n, %)	4 (6 %)	25 (39.7%)	<0.001
Dyslipemia (n, %)	6 (9 %)	24 (37.5%)	<0.001
Glucose(mg/dl)	87.3 ±9.4	94.8±15.5	<0.001
Insulin (pg/ml)	163.5±62.92	257.8± 72.1	<0.001
Leptin (pg/ml)	5486.9±3522.8	27442.1±14650.6	<0.001
Adiponectin (µg/ml)	41879.9±43959.6	17920.3± 11189.1	0.02
CRP (mg/dl)	0.15±0.35	1.15±1.08	<0.001
IL-1β (pg/ml)	0.58±0.52	1.36± 1.58	<0.001
IL-6 (pg/ml)	3.3±3.3	11.14± 11.9	<0.001
TNF-α (pg/ml)	8.7±3.8	17.02±6.92	<0.001
IL-10 (pg/ml)	38.89±26.7	37.7±23.1	0.827
MMP 9 (pg/ml)	140.8±85.9	219.9±160.8	0.004
MPO (pg/ml)	44.2±36.4	107.3±155.6	<0.001
GLP-1 (pg/ml)	21.5±8.3	21.3±6.7	0.294
GIP (pg/ml)	13.9±7.8	10.8±7.1	0.927
Ghrelin (pg/ml)	62.2±7.8	20.1±10.2	<0.001

Data values are expressed as media ± standard deviation or (%). BMI: body mass index. CRP: C reactive protein; GIP: glucose-dependent insulinotropic polypeptide; GLP-1: glucagon-like peptide-1***;*** IL: interleukin; MMP 9: metalloproteinase 9; MPO: myeloperoxidase; TNF-α: tumor necrosis factor.

Table 3. Mitochondrial proteins altered in the adipose tissue of obese patients as compared with controls identified by a proteomic analysis. 1.3-fold change cut-off for all iTRAQ ratios was selected to classify proteins as up- or down-regulated; ratio <0.77 was considered underexpressed and >1.3 was considered overexpressed.

Mitochondrial proteins	***Ratio***
10 kDa heat shock protein	**0.745**
Microsomal glutathione S-transferase	**1.482**
Aconitate hydratase	**0.735**
Enoyl-CoA hydratase	**0.697**
Electron transfer flavoprotein subunit alpha	**0.662**
Isoform Short of ES1 protein homolog	**0.711**
NADP-dependent malic enzyme	**0.738**
Protein NipSnap homolog 3A	**0.767**
Cytochrome c (Fragment)	**0.691**
T-complex protein 1 subunit zeta	**1.303**
Ras-related protein Rab-5A	**0.618**
NADH dehydrogenase [ubiquinone] flavoprotein 2	**0.698**
NADH dehydrogenase [ubiquinone] flavoprotein 1	**0.727**
Phosphoenolpyruvate carboxykinase [GTP]	**0.740**
Isoform 3 of Ethylmalonyl-CoA decarboxylase	**0.766**
Aspartate aminotransferase	**0.576**
ATPase inhibitor, mitochondrial	**1.469**

T-complex protein 1 subunit gamma	**1.369**
Branched-chain-amino-acid aminotransferase	**0.558**
Ubiquinone biosynthesis protein COQ9	**0.736**
Isoform 4 of Glutathione S-transferase kappa	**1.470**
Enoyl-CoA delta isomerase 1	**0.601**
ATP synthase lipid-binding protein	**1.363**
Other proteins	
Adiponectin	**0.681**
Collagen VI (alpha-3)	**1.359**
Protein disulfide-isomerase A6	**1.392**
Peroxiredoxin-2	**0.504**
Peroxiredoxin-5	**0.755**

Figure 1

Figure 1

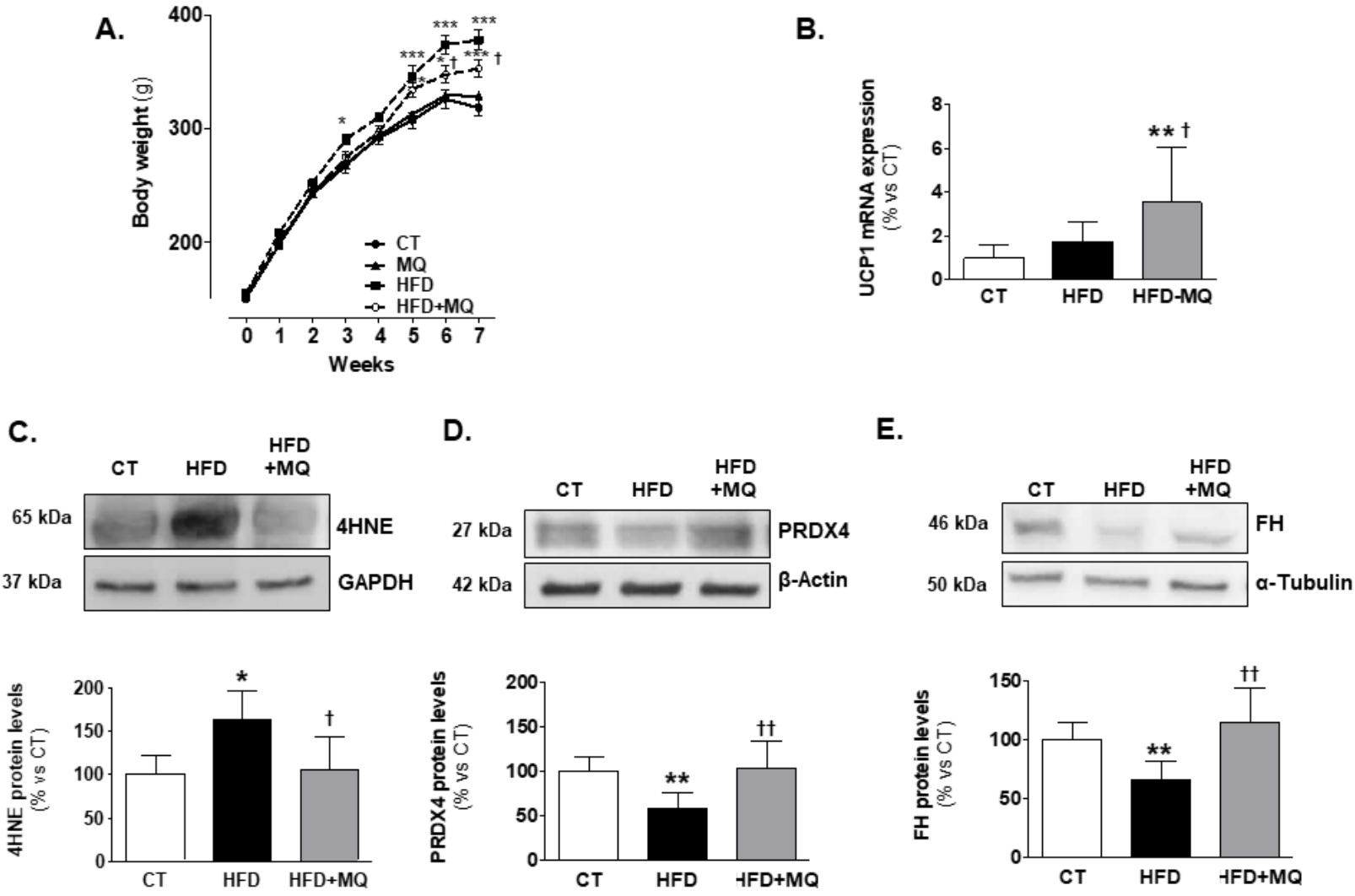

Figure 2

Figure 2

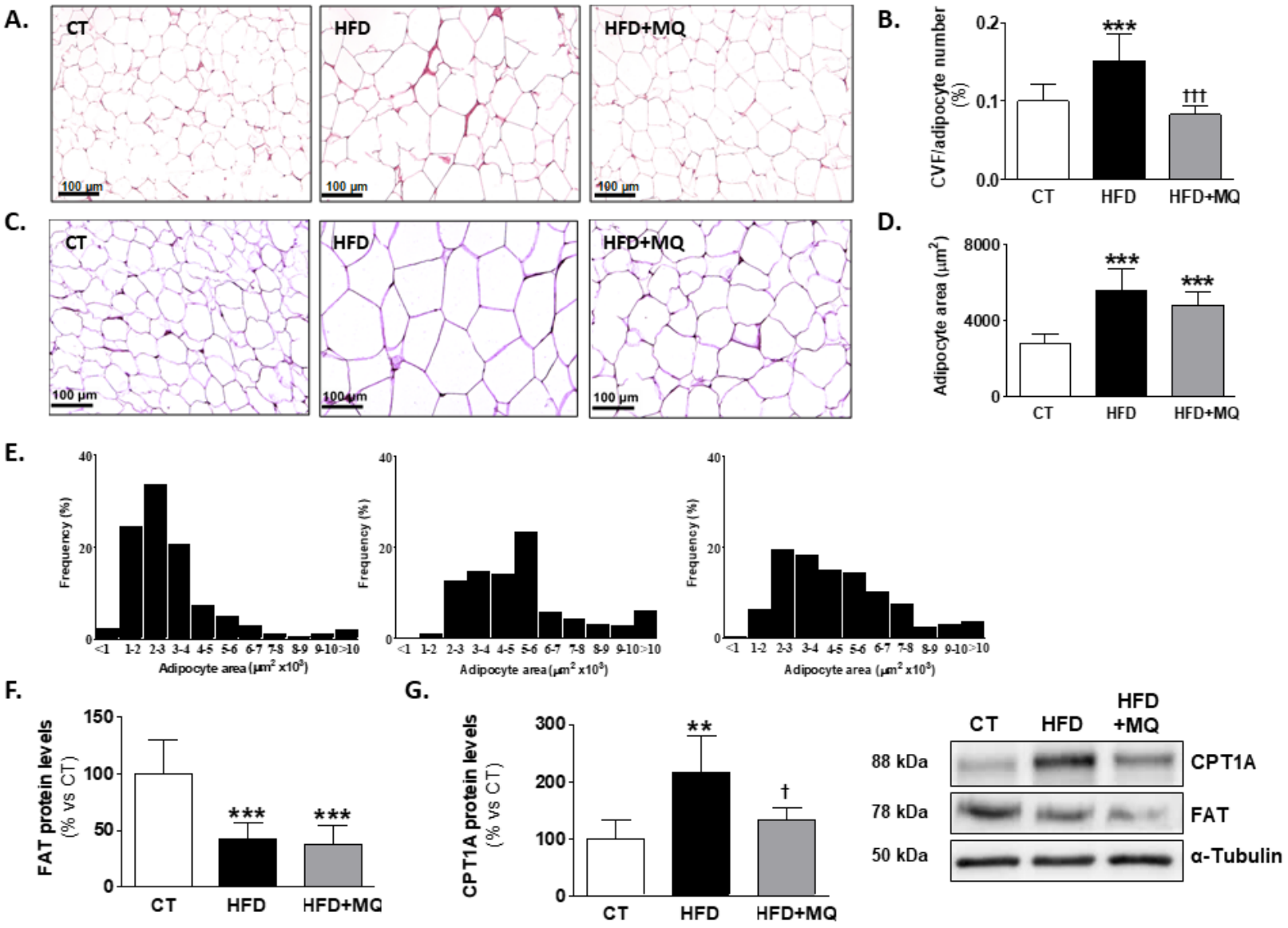

Figure 3

Figure 3

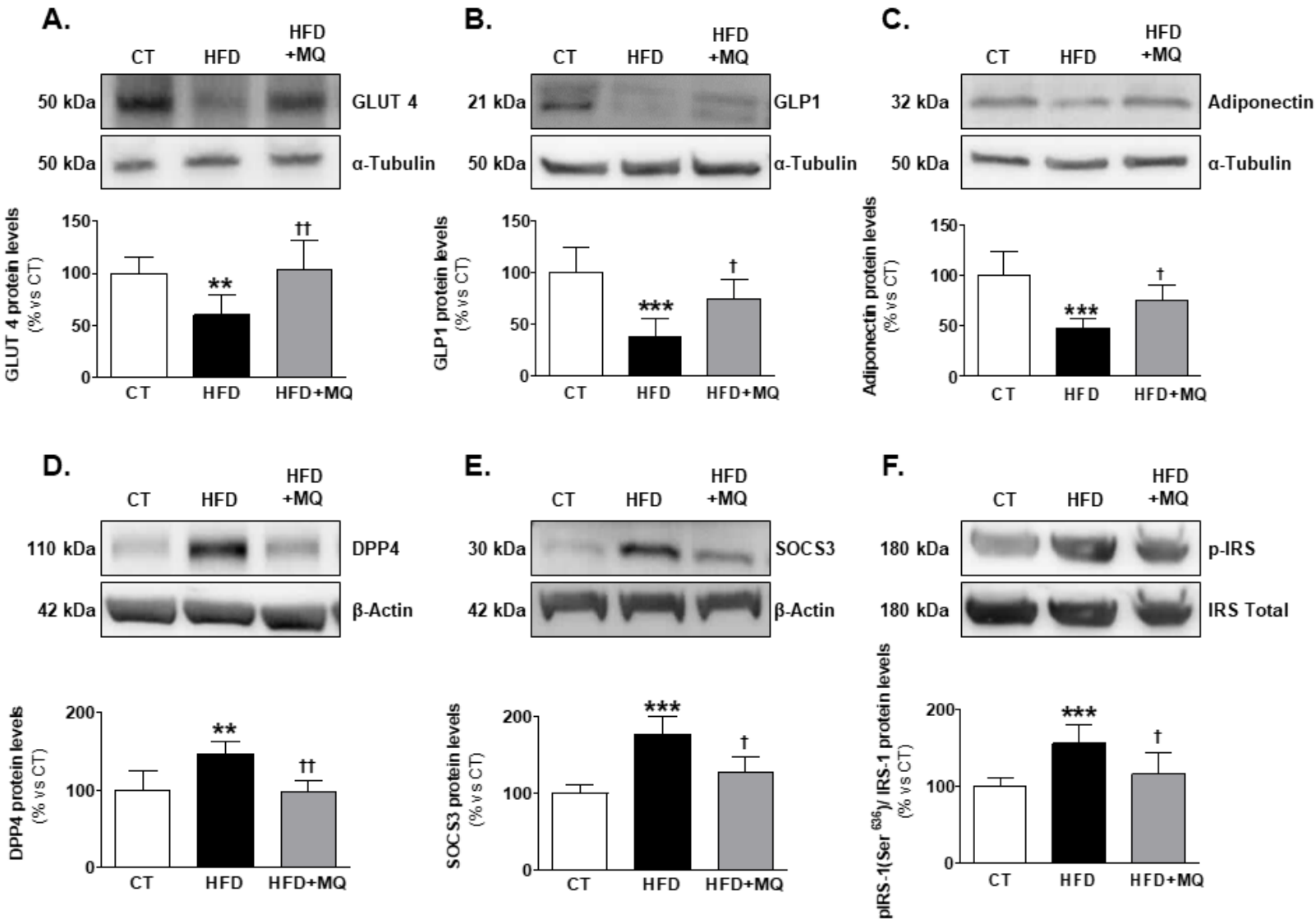

Figure 4

Figure 4

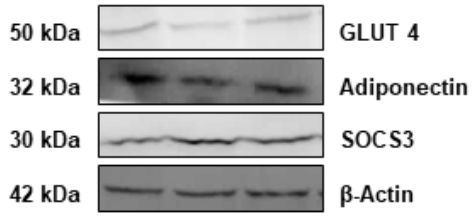

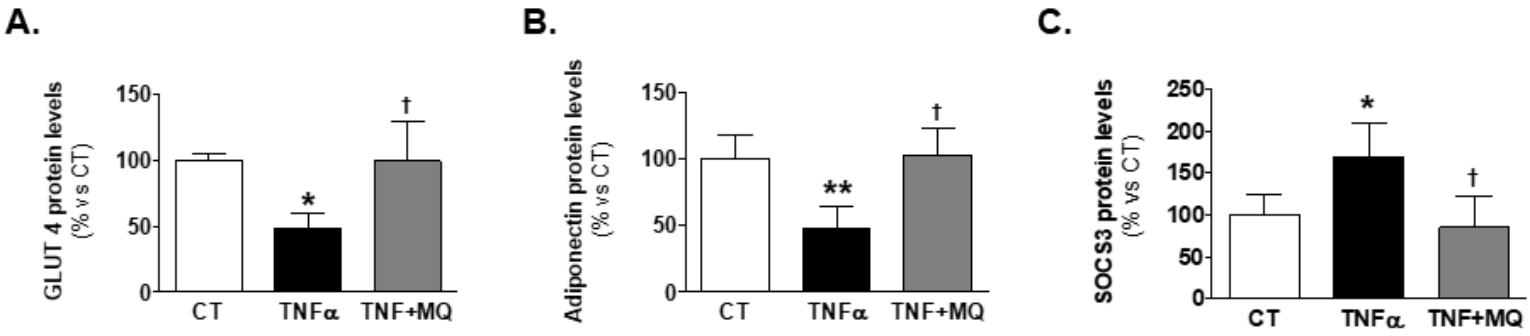

Figure 5

Figure 5

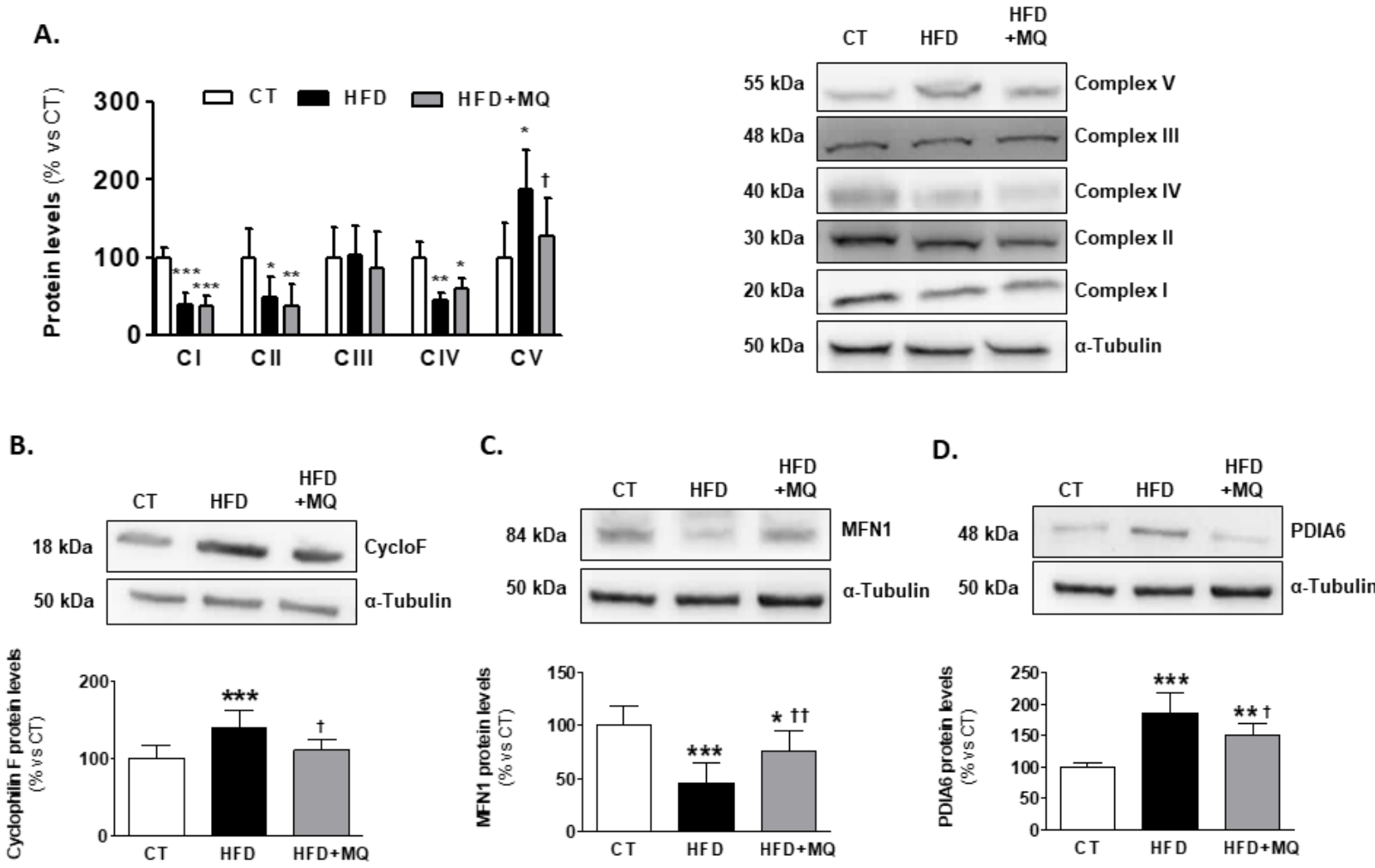

Figure 6

Figure 6